Piezoelectret sensors from direct 3D-printing onto bulk films

Youssef Sellami[1], Omar Ben Dali[1], Romol Chadda[1], Sergey Zhukov[2], Mahdi Guermazi[1], Alexander A. Altmann[1], Heinz von Seggern[2], Bastian Latsch[1], Niklas Schäfer[1], and Mario Kupnik[1]
[1] Measurement and Sensor Technology, Technical University of Darmstadt, Germany.
[2] Electronic Materials, Technical University of Darmstadt, Germany.
omar.ben_dali@tu-darmstadt.de

***Abstract*—The development of piezoelectric sensors using ferroelectrets is a very active field that is increasingly gaining importance. Recently, 3D-printing ferroelectret sensors using fused deposition modeling technique has been extensively investigated due to its unparalleled advantages in terms of design flexibility and cost-effectiveness. Nevertheless, printed structures are more rigid than bulk materials due to the minimal printable thicknesses. In this work, we present a new method that combines the advantages of 3D-printing with the high performance of bulk materials by bonding both layers in the printing process. Hereby, a polylactic acid (PLA) filament is directly printed on a 20 µm-thick bulk PLA film to form well-defined structures. This structure is thermally bonded with another PLA bulk film to form the ferroelectret. In order to enhance the sensitivity of the ferroelectrets, an additional elastomeric layer is utilized. By varying the material and thickness of the elastomeric cover, piezoelectric d_{33}-coefficients of 713 pC N^{-1} and 229 pC N^{-1} are achieved using Ecoflex™ and foamed thermoplastic polyurethane (TPU), respectively. Increasing the thickness of the Ecoflex™ cover shows a significant increase of 259 % of the piezoelectric d_{33}-coefficient.**

***Index Terms*—Ferroelectret, piezoelectret, piezoelectric sensors, 3D-printing, biodegradable.**

I. Introduction

The introduction of 3D-printing, also known as additive manufacturing, to manufacture piezoelectric sensors has significantly enhanced this field, offering unprecedented advantages in terms of design flexibility, cost-effectiveness, and rapid prototyping. 3D-printed sensors can be utilized in a wide range of applications such as robotics [1], aerospace [2], wearable sensing devices [3], [4] or medical applications [5]. These applications require sensors with specific properties, such as a complex geometry, mechanical flexibility and high sensitivity. In comparison to traditional manufacturing methods such as coating and injection molding [6], 3D printing presents a more efficient solution for manufacturing complex and precise structured sensors.

Recently, the field of 3D-printing piezoelectric sensors has been intensively investigated by using well-known piezoelectric materials such as polyvinylidene fluoride (PVDF) [7]–[9], boron nitride nanotubes (BNNTs) [10] and barium titanate ($BaTiO_3$) [11] and well known ferroelectret materials such as polypropylene (PP) [12], [13] and acrylonitrile butadiene styrene (ABS) [14]. Ferroelectrets are originally electret materials that are arranged together to form well defined air cavities. After proper treatment and polarization, such materials can exhibit piezoelectric-like behaviour reaching high piezoelectric coefficients [15]. In this context and following the urging need for eco-friendly piezoelectric materials, polylactic acid (PLA) was investigated regarding its potential to be used as ferroelectret material and showed promising results not only as cellular and bulk film but also as filament for 3D-printing [16]–[18]. The outstanding sensitivity of ferroelectrets based on bulk PLA films allowed them to be utilized as force myography sensors to detect the slightest muscle deformation on the forearm due to single fingers movements [4].

In this work, we present a new eco-friendly ferroelectret arrangement using PLA by combining the advantages of 3D-printing with those of bulk films. Hereby, the heat of the nozzle during the printing process is used to fuse the 3D-printed structure with a bulk PLA film fixed on the print bed [Fig. 1(a)]. Afterwards, an elastomeric layer is added on top of the sandwich structure to enhance the sensitivity of the ferroelectret as shown in Fig. 1(d). Such a manufacturing method offers the possibility to produce large sensors, such as a smart insole, with local properties depending on the printed thickness and geometry of the structure. However, the choice of the cover material influences the performance of the sensors significantly. Therefore, the focus of this work lies on the influence of different cover materials and their thicknesses on the sensitivity of the sensors under static loads.

II. Preparation of the Ferroelectret

The 3D-printed structure examined in this work is designed with Autodesk Fusion 360 (Autodesk, Inc.) and prepared for 3D-printing using the open source software PrusaSlicer. PrusaSlicer segments the 3D structure into layers and determines the print trajectory for the 3D-printer (Original Prusa i3 Mk3s, Prusa3d DE).

The initial step involves fixing a 20 µm-thick bulk PLA film (Maropack GmbH & Company KG, Germany) onto the print bed. The latter is heated up to 60 °C, resulting in thermal straining the bulk film. Afterwards, a circular PLA structure with an outline of 1.5 mm width and a diameter of 28 mm is

This research received support from the Deutsche Forschungsgemeinschaft (DFG) under grant no. 450821862 within the research training group 2761.

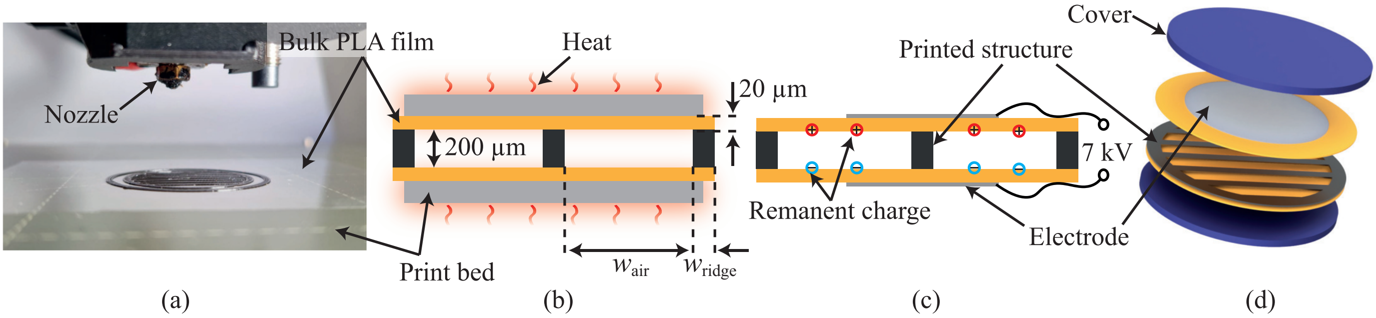

Fig. 1: Schematic representation of the ferroelectret sensor preparation process: (a) 3D-printed PLA structure on a bulk PLA film fixed onto a print bed, (b) illustration of the thermal-bonding procedure where the printed PLA structure is fused with a second bulk PLA film under a temperature of 100 °C, (c) illustration of the charging process of the ferroelectret with a poling voltage of 7 kV, (d) exploded-view of the sensor consisting of a printed PLA structure (in black) sandwich between two bulk PLA films (in orange), that form together the ferroelectret. The two outer layers represent the elastomeric covers of the sensor, which are responsible for the sensitivity of the sensor.

printed on top of the heated bulk film. Enclosed within the circle is a grid pattern consisting of multiple parallel ridges. Each ridge features a width of 1 mm and is positioned at a distance of 2 mm from the next ridge. Due to the heat of the extruded PLA filament exceeding the melting point of the bulk PLA film, the printed structure and bulk film are fused together at the contact areas. Since the printed structure is fixed on the heated print bed, the thermal strain of the bulk film remains after cooling and results in pre-stressing the bulk PLA film. The printed structure is 200 µm-thick. The printing parameters of PLA are described in a previous publication [18]. Thereafter, an additional PLA film is placed on top of the printed structure. In order to maintain the same thermal straining effect, the second PLA film is first placed on a heated print bed up to 100 °C and fused with the printed structure using thermal bonding. The grid pattern inside the circle prevents the two bulk films from collapsing into each other when exposed to 100 °C. After the bonding process, the sandwich structure together with the print beds are placed on a heatsink with a fan for accelerating the cooling process. Finally, two aluminum electrodes with a diameter of 20 mm are evaporated on both outer surfaces of the sandwich structure.

For the charging process, the electrodes are contacted with a high voltage source (HCN 14-12 500, FuG Elektronik GmbH, Germany), which applies a poling voltage of 7 kV across the sandwich structure. The electric field in the air filled voids initiates Paschen breakdown, which creates dipoles trapped at the PLA/air interfaces [19]. The charged structure is defined as a ferroelectret.

The ferroelectret is then placed between two cover layers. In this work, two different cover materials are utilized: foamed TPU (VARIOSHORE TPU NATURAL, colorFabb B.V.) and silicone rubber Ecoflex™ 00-35 (Smooth-On, Inc.).

III. Working Principle of the Ferroelectret with Elastomeric Cover

Polarizing the sandwich structure results in a permanent charge density σ_{int} within the air cavities between two printed ridges. Therefore, the maximum charge density $\sigma_{\text{int}}^{\text{max}}$ that can be trapped within the sandwich structure depends on the ratio between the width of the ridges w_{ridge} and the width of the air cavities w_{air} as [20]–[22]

$$\sigma_{\text{int}}^{\text{max}} = \frac{w_{\text{air}}}{w_{\text{air}} + w_{\text{ridge}}} \left(\varepsilon_{\text{air}} \varepsilon_0 + \varepsilon_{\text{PLA}} \varepsilon_0 \frac{t_{\text{air}}}{2 t_{\text{PLA}}} \right) E_{\text{B}}, \quad (1)$$

where E_{B} represents the electric breakdown field, ε_{air} the dielectric constant of air and t_{air} the thickness of the air gap, which corresponds to the thickness of the printed structure. The parameters t_{PLA} and ε_{PLA} are the thickness and the dielectric constant of the bulk PLA film, respectively. The piezoelectric d_{33} of such structure is known to be proportional to the charge density $\sigma_{\text{int}}^{\text{max}}$, the Young's modulus Y_{t} of the ferroelectret and the ratio of the active area to the total area as [22], [23]

$$d_{33}^{\text{max}} \propto \frac{w_{\text{air}}}{w_{\text{air}} + w_{\text{ridge}}} \cdot \frac{\sigma_{\text{int}}^{\text{max}}}{Y_{\text{t}}}. \quad (2)$$

However, increasing w_{air} leads to a smaller bending stiffness and results in a pull-in while charging the structure due to the electrostatic forces. Therefore, a ratio of $w_{\text{air}}/w_{\text{ridge}} = 2/1$ is selected.

The piezoelectric behaviour of ferroelectrets generally originates from the deformation of the air-cavities, causing the dipoles in the air to move closer to each other [24], [25]. Due to the rigidity of the printed PLA structure, applying a force to the ferroelectret itself results in low piezoelectric d_{33}-coefficients in the range of few pC/N. In order to enhance the deformation of the air cavities, an additional elastomeric layer is added on top of the ferroelectret to reduce the apparent

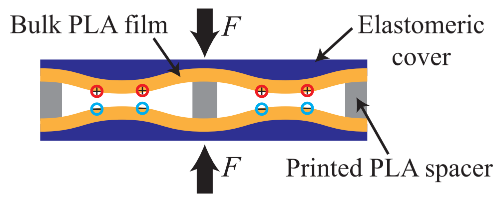

Fig. 2: Schematic representation of the deformation of the ferroelectret due to an external force F, when using an elastomeric cover.

Young's modulus as introduced by Mirkowska [26]. Applying a force to the elastomeric cover leads to a more concentrated deformation of the less rigid part of the ferroelectret, which corresponds to the air cavities as shown in Fig. 2. Depending on the thickness and the material used as cover, the sensitivity of the ferroelectret can be increased significantly.

IV. Experimental Results and Discussion

The dependency of the piezoelectric d_{33}-coefficient of the sensor on the cover material is measured by means of a setup consisting of a linear guide and an electrometer. The linear guide prevents an uneven application of force to the sensor and ensures the same pressure area regardless of the utilized mass. Furthermore, the sensor is pre-stressed with the mass of the linear guide of 27 g, which prevents undesired motion of the sensor while placing and removing the measurement load. The pressure area of the linear guide is approximately 314 mm^2 which corresponds to a diameter of 20 mm. Since the diameter of the used electrode corresponds to the diameter of the pressure area, the piezoelectric d_{33}-coefficient can be determined as

$$d_{33} = \frac{Q}{F} = \frac{Q}{m\ g}, \tag{3}$$

where Q is the induced charge on the electrodes, F is the force applied to the sensor caused by the mass m placed on the linear guide and g is the gravitational acceleration.

First, a force is applied on the linear guide for a substantial period of time of 1 min. The charge induced after removing the mass is measured by means of an electrometer (6517A, Keithley Instruments) and integrated over 10 s. This process is repeated with different mechanical loads ranging from 1 N to 10 N.

By utilizing an Ecoflex™ 0.5 mm-thick cover, a piezoelectric d_{33}-coefficient of 275 $pC\,N^{-1}$ is achieved [Fig. 3(a)]. Increasing the applied force results in a small decrease of piezoelectric d_{33}-coefficient to reach a value of 214 $pC\,N^{-1}$ starting from a force of 3 N. This value is then maintained even by further increasing the applied force up to 10 N. Increasing the thickness of the Ecoflex™ cover, however, leads to a significant improvement of the piezoelectric d_{33}-coefficient. Under a load force of 1 N, an enhancement of 174% corresponding to 479 $pC\,N^{-1}$ for a 1 mm-thick cover is recorded. Further increasing the thickness to 1.5 mm leads to an enhancement of 259% corresponding to a value of 713 $pC\,N^{-1}$ [Fig. 3(a)].

This effect can be explained by the fact that increasing the thickness of the silicone rubber Ecoflex™ leads to a smaller effective stiffness of the cover, since the same force results in a larger displacement. Furthermore, the more material is pressed into the cavities of the ferroelectret structure, the more charge is induced on the electrodes leading to larger d_{33}-coefficients.

On the other hand, using a foamed TPU cover leads to smaller d_{33}-coefficients. In fact, applying a load of 1 N results in d_{33}-coefficients between 173 $pC\,N^{-1}$ and 229 $pC\,N^{-1}$ for thicknesses between 0.5 mm and 1.5 mm, respectively. The d_{33}-coefficients, however, decrease gradually with increased loads, reaching a value of 112 $pC\,N^{-1}$ for a load force of 10 N. In contrast to the Ecoflex™ cover, for a larger foamed TPU thickness only smaller d_{33}-coefficients have been recorded [Fig. 3(b)]. Considering that increasing the thickness of the foamed TPU results in a stiffer cover, the consequence of smaller d_{33}-coefficients becomes evident.

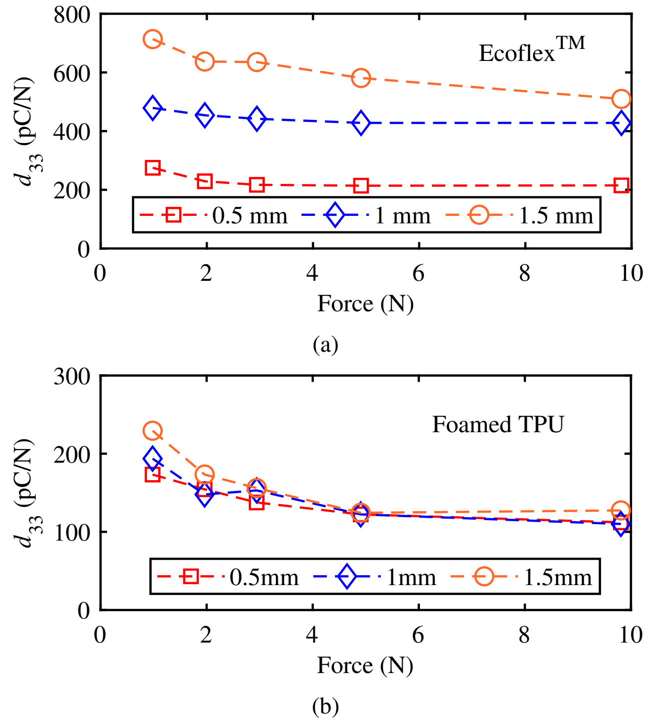

Fig. 3: Quasi-static measurements of the piezoelectric d_{33} coefficient for different cover thicknesses using (a) Ecoflex™ and (b) foamed TPU. All measurements correspond to the average values measured for ten different sensors.

V. Conclusion and Outlook

In this work, a manufacturing technique involving the combination of 3D-printing and bulk PLA film is presented. Directly 3D-printing a PLA structure onto a bulk PLA film fixed on the print bed leads to their fusion during the printing process. By using an additional elastomeric cover consisting of Ecoflex™ on top of the ferroelectret, large piezoelectric d_{33}-coefficients up to 713 $pC\,N^{-1}$ are achieved. Furthermore, the dependency of the d_{33}-coefficients on the cover material and thickness is demonstrated. This simple manufacturing technique broadens the possibility of manufacturing ferroelectrets by combining filament with bulk films as soon as they are of the same materials, whether PP, ABS or any other known electret material. The utilized 3D-printer in this work allows the manufacturing of sensors featuring an area of 200 mm $\times$ 200 mm, which corresponds to the area of the print bed. Alternatively, this surface can be used to print multiple smaller sensors on the same bulk PLA film. Since the PLA and the Ecoflex™ are bio-compatible materials, these sensors are appropriate for medical applications as well.

References

[1] J. Zhang, S. Ye, H. Liu, *et al.*, "3d printed piezoelectric bnnts nanocomposites with tunable interface and microarchitectures for self-powered conformal sensors," *Nano Energy*, vol. 77, p. 105 300, 2020.

[2] S. Bodkhe, G. Turcot, F. P. Gosselin, and D. Therriault, "One-step solvent evaporation-assisted 3d printing of piezoelectric pvdf nanocomposite structures," *ACS applied materials & interfaces*, vol. 9, no. 24, pp. 20 833–20 842, 2017.

[3] O. B. Dali, Y. Sellami, S. Zhukov, *et al.*, "Ultrasensitive and low-cost insole for gait analysis using piezoelectrets," in *2022 IEEE Sensors*, IEEE, 2022, pp. 1–4.

[4] O. Ben Dali, S. Zhukov, R. Chadda, *et al.*, "Eco-friendly high sensitive piezoelectrets for force myography," *IEEE Sensors Journal*, vol. 23, no. 3, pp. 1943–1951, 2023.

[5] D. Grinberg, S. Siddique, M.-Q. Le, R. Liang, J.-F. Capsal, and P.-J. Cottinet, "4d printing based piezoelectric composite for medical applications," *Journal of Polymer Science Part B: Polymer Physics*, vol. 57, no. 2, pp. 109–115, 2019.

[6] Y. Jiang, M. N. Islam, R. He, *et al.*, "Recent advances in 3d printed sensors: Materials, design, and manufacturing," *Advanced Materials Technologies*, vol. 8, no. 2, p. 2 200 492, 2023.

[7] H. Kim, F. Torres, Y. Wu, D. Villagran, Y. Lin, and T.-L. B. Tseng, "Integrated 3d printing and corona poling process of pvdf piezoelectric films for pressure sensor application," *Smart Materials and Structures*, vol. 26, no. 8, p. 085 027, 2017.

[8] X. Liu, J. Liu, L. He, Y. Shang, and C. Zhang, "3d printed piezoelectric-regulable cells with customized electromechanical response distribution for intelligent sensing," *Advanced Functional Materials*, vol. 32, no. 26, p. 2 201 274, 2022.

[9] A. Kumar, D. Saini, and D. Mandal, "3d printed ferroelectret with giant piezoelectric coefficient," *Applied Physics Letters*, vol. 120, no. 18, p. 182 901, 2022.

[10] J. Zhang, S. Ye, H. Liu, *et al.*, "3d printed piezoelectric bnnts nanocomposites with tunable interface and microarchitectures for self-powered conformal sensors," *Nano Energy*, vol. 77, p. 105 300, 2020.

[11] H. Kim, F. Torres, D. Villagran, C. Stewart, Y. Lin, and T.-L. B. Tseng, "3d printing of batio3/pvdf composites with electric in situ poling for pressure sensor applications," *Macromolecular Materials and Engineering*, vol. 302, no. 11, p. 1 700 229, 2017.

[12] Y. A. Assagra, R. A. Altafim, J. P. do Carmo, *et al.*, "A new route to piezo-polymer transducers: 3d printing of polypropylene ferroelectrets," *IEEE Transactions on Dielectrics and Electrical Insulation*, vol. 27, no. 5, pp. 1668–1674, 2020.

[13] N. Wang, K. Davis, M. Sotzing, *et al.*, "Flexible nanogenerator with 3d-printed ferroelectrets," in *2021 IEEE Conference on Electrical Insulation and Dielectric Phenomena (CEIDP)*, IEEE, 2021, pp. 375–378.

[14] I. Kierzewski, S. S. Bedair, B. Hanrahan, H. Tsang, L. Hu, and N. Lazarus, "Adding an electroactive response to 3d printed materials: Printing a piezoelectret," *Additive Manufacturing*, vol. 31, p. 100 963, 2020.

[15] X. Qiu, Y. Bian, J. Liu, *et al.*, "Ferroelectrets: Recent developments," *IET Nanodielectrics*, vol. 5, no. 3-4, pp. 113–124, 2022.

[16] X. Ma, S. Zhukov, H. von Seggern, *et al.*, "Biodegradable and bioabsorbable polylactic acid ferroelectrets with prominent piezoelectric activity," *Advanced Electronic Materials*, vol. 9, no. 3, p. 2 201 070, 2023.

[17] O. Ben Dali, S. Zhukov, M. Rutsch, *et al.*, "Biodegradable 3d-printed ferroelectret ultrasonic transducer with large output pressure," in *2021 IEEE International Ultrasonics Symposium (IUS)*, IEEE, 2021, pp. 1–4.

[18] O. Ben Dali, S. Zhukov, C. Hartman, H. von Seggern, G. M. Sessler, and M. Kupnik, "Biodegradable additive manufactured ferroelectret as mechanical sensor," in *2021 IEEE Sensors*, IEEE, pp. 1–4.

[19] B. Crichton, "Gas discharge physics," in *IEE Colloquium on Advances in HV Technology*, 1996, pp. 3/1–3/5.

[20] B.-X. Xu, H. von Seggern, S. Zhukov, and D. Gross, "Continuum modeling of charging process and piezoelectricity of ferroelectrets," *Journal of Applied Physics*, vol. 114, no. 9, p. 094 103, 2013.

[21] H. von Seggern, S. Zhukov, and S. Fedosov, "Importance of geometry and breakdown field on the piezoelectric d_{33} coefficient of corona charged ferroelectret sandwiches," *IEEE Transactions on Dielectrics and Electrical Insulation*, vol. 18, no. 1, pp. 49–56, 2011.

[22] H. von Seggern, S. Zhukov, O. Ben Dali, C. Hartmann, G. M. Sessler, and M. Kupnik, "Highly efficient piezoelectrets through ultra-soft elastomeric spacers," *Polymers*, vol. 13, no. 21, p. 3751, 2021.

[23] S. Zhukov, D. Eder-Goy, S. Fedosov, B.-X. Xu, and H. von Seggern, "Analytical prediction of the piezoelectric d_{33} response of fluoropolymer arrays with tubular air channels," *Scientific reports*, vol. 8, p. 4597, 2018.

[24] S. Bauer, "Piezo-, pyro-and ferroelectrets: Soft transducer materials for electromechanical energy conversion," *IEEE Transactions on Dielectrics and Electrical Insulation*, vol. 13, no. 5, pp. 953–962, 2006.

[25] O. Ben Dali, S. Zhukov, R. Chadda, *et al.*, "Modeling of piezoelectric coupling coefficients of soft ferroelectrets for energy harvesting," in *2019 IEEE International Ultrasonics Symposium (IUS)*, IEEE, 2019, pp. 2454–2457.

[26] A. Mirkowska, R. Kacprzyk, and K. Rozmaryniewicz, "Piezoelectric structure with a 3-d printed mesh layer," *IEEE Transactions on Dielectrics and Electrical Insulation*, vol. 29, no. 3, pp. 823–828, 2022.